Energy Conversion and Management 293 (2023) 117498

Contents lists available at ScienceDirect

Energy Conversion and Management

journal homepage: www.elsevier.com/locate/enconman

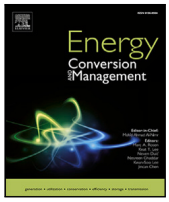

Effect of differential control and sizing on multi-FCS architectures for heavy-duty fuel cell vehicles

R. Novella, J. De la Morena, M. Lopez-Juarez *, I. Nidaguila

CMT-Motores Térmicos, Universitat Politècnica de València, Camino de vera s/n, 46022 Valencia, Spain

ARTICLE INFO

Keywords:
Hydrogen
Proton exchange membrane fuel cell
Heavy duty vehicle
Driving cycle
Differential control
Durability

ABSTRACT

The current trend towards a zero-emission transport sector has increased the interest of the scientific community and the industry in fuel cell (FC) technologies in the past few years. Previous studies have focused on passenger car analyses to differentiate them from the current battery electric vehicle (BEV) alternative. However, deploying these technologies may be even more critical for the transportation-produced global emissions if they are used in different applications, such as heavy-duty commercial vehicles. This study uses a differential control strategy to find the best fuel-cell performance for a heavy-duty vehicle application. In addition, and as a differentiation point from other studies in the literature, this article exploits the modularity of the heavy-duty truck sector to implement a design with optimal fuel cell system (FCS) sizing and control dynamics distribution in terms of durability and H_2 consumption. Low dynamics could increase 471% in durability just for a 3.8% increase in H_2 consumption. When using a multi-FCS with non-equal power FCS, a high dynamics behavior of the small FCS significantly improves the durability for a small consumption penalty (less than 0.7%). The obtained data has proven that the combination of these two design strategies shows an improved vehicle performance that could lead to environmental impact and cost reduction, which is significant in the current development stage of fuel cell vehicle (FCV) technologies.

1. Introduction

In the present times, the current global warming crisis is leading transportation technologies towards a zero emissions trend [1] in each of the different sectors, including road [2], aerial [3], and maritime [4]. From the total amount of the CO_2 emissions produced in 2020 by this sector, around 77% came from on-road vehicles [5]. Heavy-duty vehicles represent 30% of the mentioned transport-produced emissions. In addition, the contribution of these emissions to climate change and air pollution is very high compared to their relative numbers in the global vehicle fleet. This is because of their substantial particulate matter emissions, including black carbon, which has short-term warming potential [5].

In this framework, hydrogen FCS has proved to be one of the critical technologies to solve the carbon emissions problem in the automotive sector. Nowadays, most roadmaps that aim to achieve the zero-emission objective, both in an individual state [6] and global [7] framework, present hydrogen as one of the solutions to reduce greenhouse gas emissions (GHG). The main advantage of H_2 as a power source is its zero CO_2 emissions, both when burnt or used in an FCS. Its advantage over other non-pollutant energy carriers is its high energy density. H_2 allows mitigating the energy imbalances produced by renewable energy. When studying in detail the lifecycle emissions for near-future situations, it has been proven that to reduce GHG, H_2 and electric technologies should be used together with the appropriate energy mix to minimize the environmental impact of the road transport [8].

Fuel cell trucks are already being developed and presented as a promising solution to decarbonize the heavy-duty vehicle fleet [9]. There have already been some significant experiences with FC buses with promising results [10]. This kind of heavy-duty vehicle is a good starting point since public transport subsidies ease the deployment of new technologies and can be used to check the benefits of FCS in heavy-duty. However, buses only represent a 4% of the actual carbon emissions concerning the 30% of heavy-duty commercial vehicles [5].

Other low-carbon technologies, such as electric vehicles, are disadvantaged compared to the FC truck solution [11]. Fuel cell systems have a much higher gravimetric and volumetric energy density than lithium-ion battery packs. Even when considering the weight of the auxiliary electric battery, the gravimetric energy density of an FCV is three times higher than in a BEV [12]. Therefore, the main problem of BEVs compared to FCVs comes when used intensively. High energy storage

* Corresponding author.
E-mail address: marlojua@mot.upv.es (M. Lopez-Juarez).
URL: http://www.cmt.upv.es (M. Lopez-Juarez).

https://doi.org/10.1016/j.enconman.2023.117498
Received 29 March 2023; Received in revised form 31 July 2023; Accepted 1 August 2023
Available online 18 August 2023

Glossary

BEV	Battery Electric Vehicle
BoP	Balance of plant
CAPEX	Capital expenditure
DP	Dynamic Programming
ECMS	Equivalent Consumption Minimum Strategy
EMS	Energy Management Strategy
FC	Fuel Cell
FCS	Fuel Cell System
FCV	Fuel Cell Vehicle
GHG	Greenhouse Gas
HD	Heavy-duty
HDDT	Heavy-duty Diesel Truck
HDFCV	Heavy-duty Fuel Cell Vehicle
HEV	Hybrid Electric Vehicle
LCA	Lifecycle assessment
OC	Optimal Control
OPEX	Operational Expenditure
PMP	Pontryagin Minimum Principle
SOC	State-of-charge
TCO	Total Cost of Ownership

is required for this purpose, translating into a higher battery mass and cost. This increment means a lower load capacity and higher energy consumption. Furthermore, recharging time would also be higher, and reducing it would create instabilities in the electric network and degrade the battery at a higher rate. Therefore, it would be hard for BEV [13] to satisfy the heavy-duty market segment. In [14], Yan et al. research a possible deployment of FCV and BEV, concluding that the FC solution is more appropriate for the heavy-duty (HD) transportation sector. Thus, looking into the FC propulsive solution could benefit market trends and global research objectives.

Comparing FCS with conventional diesel heavy-duty trucks shows that efficiency and cost still need to be improved [15]. Finding the optimal component sizing distribution for FC powertrains will allow the improvement of these technologies. Thus, a sizing analysis is performed in the present study.

1.1. Discussion of previous works

The interest in FCS as a research topic in the transportation sector raised in the last decade and has increased over the previous years. This comes from the need for the decarbonization of these technologies. Due to the lack of knowledge in the field, in most cases, the performed studies aim to understand the global characteristics of the performance of the vehicle. This has led to using simple FCS models or ones focusing on one specific system aspect. For example, in [16], Kim et al. focus on the BoP and do not consider degradation mechanisms. Besides, in [17], Li et al. focus on the FCS and battery degradation using a simplified FCS model. In addition, this degradation model does not account for aspects such as the effect of temperature or relative humidity. Finding an extensive and precise degradation model for FCS in the literature is hard.

Hybrid Electric Vehicles (HEV) represent the transition between current and future powertrains to solve the zero-emissions issue. The performed studies with this type of vehicle are highly interesting, as the proposed FCHDV also contains an electric battery. Thus, some FC vehicles can be considered hybrids.

A common trend in HEV is to study different vehicle topologies, as Xu et al. do in [18]. These different topologies include the distribution of the powertrain components in the vehicle but also the choice of the various elements to implement the propulsive system. In [19], Morozov et al. compare different power e-motors and gearboxes, and in [20], Verbruggen et al. also consider different battery sizes and control strategies.

As FCVs are being developed, research in the field keeps increasing. Firstly, the performed studies focused on the feasibility of these technologies in a simple way. In [21], Kast et al. compared different MD and HD standardized vehicles with their desired range to understand their viability. In addition, the analyses made in this kind of hybrid usually focus on optimizing the EMS [22].

In previous passenger car studies, different control strategies have been used to optimize the performance of the system. In [23], Ravey et al. compare offline and online control strategies. In this case, the chosen offline control strategy is dynamic programming (DP), which optimizes fuel consumption, knowing the driving cycle that the vehicle will perform. The online controller uses genetic algorithms and offline results to tune its behavior. Thus, a deeper analysis of offline control strategies should be done before using them to train online control strategies. In [24], Xu et al. explain that the problem of using the DP strategy in real-time decision-making solutions is a long time taken and the large amount of data needed to store results. In this paper, a comparison between DP, the Pontryagin Minimum Principle (PMP), and the Equivalent Consumption Minimization Strategy (ECMS) is made and leads to the choice of a strategy between PMP and ECMS rather than DP, which maximizes performance in terms of the selected variable.

In the case of the HD market, in [25] Ferrara et al. compare different energy management strategies (EMS) and try to optimize the lifetime of the system while also reducing hydrogen cost for a 300 kW FCS and an additional battery.

In [26], Peng et al. study different power rates for the FCS for the railway sector. The dynamics of the system have an impact on the durability of the FCS. However, controlling them using the current density change instead of the power could be beneficial. The current density is a value that does not depend on the power of the FCS, thus, a standard FCS parameter. Li et al. analyze the optimal way to change the current density to extend the life of the FCS in [27]. This study uses a battery and a supercapacitor to supply the required energy while changing the current density rate of the FCS to its optimum. However, these auxiliary elements would not be necessary for an HDV with 2 FCS with different dynamic strategies.

The current sizing studies for HDFCV found in the literature test a battery and FCS distribution and try to optimize a chosen aspect (lifetime, consumption, cost, etc.). In [28], Jain et al. compare different powertrain designs for buses composed of an FCS, an electric battery, and an ultracapacitor in terms of consumption and cost. In addition, Anselma et al. present in [29] a study of the actual and future FCV cost. This analysis shows a high amount of different-size designs, but they are all composed of one FCS and an electric battery.

One of the advantages of FC powertrains in heavy-duty applications is their modularity. In [30], Peng et al. look into a multi-FCS for heavy-duty applications with 110 kW FCS. Thus, finding the optimal power arrangement for the FCS included in the vehicle would be interesting. However, the actual FC truck trend shows an equal-power FCS architecture [31]. Therefore, a powertrain with two different fuel cell sizes and an electric battery has not been analyzed, and it would represent research of high novelty.

The actual sizing analyses study the H_2 consumption since this parameter is an excellent value to measure performance efficiency and cost [32]. Thus, quantifying the consumption depending on the power of each FCS could be very helpful for transportation sector manufacturers to find the optimal distribution for each application. In addition, the production cost is also essential when trying to understand the total cost of any powertrain. Therefore, the relation between the size of the components and their lifetime could help to find the optimal arrangement. A realistic estimation of the life of the FC would also

be very valuable when performing a study of the produced emissions or life cycle analysis. In [33], Cox et al. make a comparative study in terms of cost (TCO) and emissions (LCA). However, the durability data used comes from other studies or simple models; a dedicated durability calculation should be used to increase the reliability of the analysis.

In summary, the existing literature shows that there is not much research on HDFCV. However, in the last years, the interest has significantly increased. In addition, hybrid-related papers can be used to set a basis for the desired characteristics of interest. Moreover, the existing studies focus on modeling one component or phenomenon acting on the FCS. Therefore, they tend to be simple.

In the HD sector, a modularity trend in design is starting to gain research weight. However, this interest is relatively recent, and, for now, no studies analyze the effect of different sizes or dynamics of FCS on the vehicle.

1.2. Approach of the authors

Firstly, it is essential to consider the segment of the transportation sector being studied. Nowadays, there exists a considerable amount of passenger car sizing and control strategy studies [34]. However, the HD field has different power and weight requirements that would influence the results and, thus, need a dedicated study. Moreover, the dynamics followed by a truck on its usual driving cycle are very different from other vehicles, which would also impact the final results.

The existing literature shows increasing research on FCS for HD applications. However, there is still much work before these propulsive systems are used as a vehicle solution. The present study has been carried out so the HD industry can practically use the results. This means it gives an overview of the vehicle rather than focusing on a specific aspect, such as most reviewed previous works.

The present research provides significant novelty concerning the existing work:

- FCV model based on an HD vehicle and including the BoP, a complex degradation model, and an EMS that optimizes its performance. The used platform integrates a complete vehicle with a significant amount of detail compared to other literature models. As expected, this precision increases the level of complexity of the performed study. Besides, this detail increment is considered a necessary step at the research point FCS are at the present times.
- Semi-empirical degradation model that is based on significant degradation mechanisms that act on an FCS, which represents an improvement from the existing degradation models that focus on some specific phenomena. Furthermore, the present model has been designed and calibrated to work under driving cycle conditions.
- Modular powertrain design that represents the most recent HD-FCV market trends. FCS have recently been introduced to the HD market, thus, research in this field is still rare.
- Different sizes of the FCS that compose the propulsive system. This kind of sizing strategy has not been explored yet and can represent undiscovered knowledge for HDFCV manufacturers.
- An EMS that optimizes the performance of the vehicle, together with different current density rate of change of each FCS. The literature reviewed results such as [35] show how PMP can be used to improve the performance of the battery-fuel cell system and is the right control strategy to benchmark different architectures. Thus, the present study used this EMS to test how a differential control strategy between the two different FCS would influence lifetime and performance.

1.3. Knowledge gaps

Considering the available data and studies in the literature, the present study covers some of the existing knowledge gaps in the fuel cell heavy-duty commercial vehicle sector.

1. Heavy-duty commercial vehicles work under very different conditions than passenger cars. As a starting point for further studies, the performance variation that a differential control strategy induced in HDDT (Heavy-Duty Diesel Truck) driving cycle conditions for the simplest case, a combination of two equal-power FCS, needs to be quantified. This performance change has not been correlated to the consequence H_2 consumption penalty.
2. The modularity characteristic of FCS in heavy-duty applications has not been analyzed in deep detail yet. Therefore, the influence of differential FCS sizing has not been assessed.
3. The impact in consumption of differential sizing and differential control strategies has been studied for passenger cars and heavy-duty applications in terms of battery-fuel cell combinations. However, this is still a field in which analyses have not been performed regarding different power FCS.
4. The existing degradation models for fuel cell vehicle applications have already been used to evaluate heavy-duty durability. However, the lifetime of a modular FC powertrain for trucks has not been quantified, particularly when considering differential control.
5. The differential control strategy represents a novel and new methodology. Thus, it is still unclear if changing the dynamic behavior of one FCS will represent a variation in the durability of the other FCS.

From the previous considerations, it is evident how the effect on durability and performance of a different power FCS combination has never been studied. In addition, combining this kind of architecture with a differential control strategy would provide an understanding of an unexplored field.

To give an overview of the commented literature and the situation of the present paper, Tables 1–3 summary the advantages of the performed analysis.

1.4. Contribution and objectives

The main objective of this paper consists of understanding how differential sizing and a differential control strategy would influence performance and durability in a combined FCS heavy-duty truck. The specific contributions to achieving such an objective are:

- Measure the influence of a differential control and sizing strategy on the performance of the system, measured by its hydrogen consumption.
- Check how the FC durability changes depending on the maximum rate of change of the current density and difference FCS power distributions.
- Find the trade-off between H_2 consumption and performance using differential control and sizing strategies.
- Optimize the powertrain solution by combining the effect of a differential sizing and control strategy.

The accomplishment of the previously stated tasks would lead to the achievement of the final goal of this study and filling the current knowledge gaps in the field (Section 1.3).

2. Methodology

The effect of FC stack sizing and dynamic limitations on performance and durability was analyzed by performing a set of simulations on a validated FC-based powertrain. The optimization of the balance of plant components had already been carried out during previous studies to maximize FCS efficiency [36]. The resulting model was integrated into a heavy-duty fuel cell vehicle (HDFCV) architecture. In addition, to simulate the HDDT driving cycle in realistic conditions,

Table 1
Existing literature reviewed, part 1.

Ref.	Title	Recent study (<5 years)	Year	Basic approach and methods	Limitations
[16]	Establishment of energy management strategy of 50 kW PEMFC hybrid system	Yes	2023	BoP detailed design. Simulations performed with a MATLAB-Simulink FC and battery model based on experimental data from other literature sources.	Does not consider degradation
[17]	Cost Minimization Strategy for Fuel Cell Hybrid Electric Vehicles Considering Power Sources Degradation	Yes	2020	Degradation of the FCS and battery. FC models based on theoretical models.	Simplified FCS model. Does not cover degradation mechanisms as temperature or humidity.
[18]	A Comparative study of Different Hybrid Electric Powertrain Architectures for Heavy-Duty Truck	No	2018	Different vehicle topologies for a HEV and different propulsive systems. Simulations developed in an own model validated with experimental data.	No FCS involved. Shows the current studied market trends for hybrid vehicles.
[19]	Design, Analysis, and Optimization of a Multi-Speed Powertrain for Class-7 Electric Trucks	No	2018	Different e-motors and gearboxes for HEV.	No FCS involved. Shows the current studied market trends for hybrid vehicles.
[20]	Electric Powertrain Topology Analysis and Design for Heavy-Duty Trucks	Yes	2020	Different battery sizes and control strategies for HEV. The simulations have been done with MATLAB and VECTO.	No FCS involved. Shows the current studied market trends for hybrid vehicles.
[21]	Clean commercial transportation: Medium and heavy duty fuel cell electric trucks	No	2017	Comparison of MD and HD vehicles with their desired range. Vehicles simulated with Argonne National Laboratory Autonomie Model.	Uses predefinied automotive software to simulate the vehicles.
[22]	Optimization of Energy Management Strategy for Fuel Cell Hybrid Electric Vehicles Based on Dynamic Programming	Yes	2022	Optimization of the EMS. FCHV modeled in MATLAB-Simulink and experimentally validated.	Passenger car optimization using DP. Changes dynamics but not the sizing of the powertrain.
[23]	Control Strategies for Fuel-Cell-Based Hybrid Electric Vehicles: From Offline to Online and Experimental Results	No	2012	Comparison of online and offline control strategies.	Simple vehicle model.

energy management optimizer algorithms and semi-empirical degradation models [37] were also developed and integrated into the system. All the significant parts of the modeling procedure used are explained in this section. However, the main focus of this explanation is on the HDFCV architecture, which represents the novelty of this study. The FC stack model, the management of the balance of plant architecture, and the degradation model were performed in previous studies, and, therefore, their explanation can be found in deeper detail in them [36–38].

The vehicle model was developed in GT-Suite v2020. This software is a powerful numerical tool that can be used to model 0D-1D thermal fluid dynamics. In order to understand the behavior of the modeled dynamics, it numerically solves the continuity, momentum, energy, and species equation and applies common physically-based correlations. This platform is widely used in the automotive industry and for research and development. This tool also allows connections from other software; therefore, two different MATLAB R2022a models are used to integrate the degradation model and the energy management strategy optimizer in the system.

Fig. 1 shows a flow chart aimed to ease the understanding of the performed study. The diagram presents the methodology used through the paper in a sequenced way to give an overview of the process before explaining in detail each part of the process.

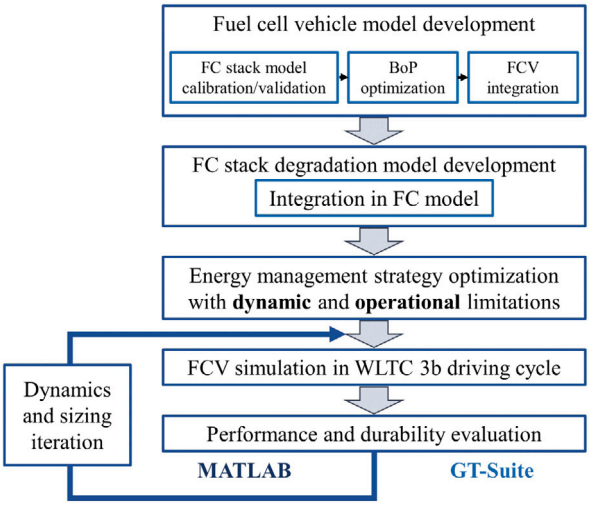

Fig. 1. Methodology flow chart.

2.1. Fuel cell vehicle model

The FCV model can be differentiated into two separate models. On the one hand, the vehicle architecture comprehends the characteristics of the simulated vehicle, but also the battery. Ideally, a different and more detailed battery model could be used. However, since the most important part of the actual study is the FCS distribution, such a level of detail is not necessary for the battery. On the other hand, an FCS model is used to understand the FC in the most precise way possible.

Table 2
Existing literature reviewed, part 2.

Ref.	Title	Recent study (<5 years)	Year	Basic approach and methods	Limitations
[24]	Application of Pontryagin's Minimal Principle to the energy management strategy of plugin fuel cell electric vehicles	No	2013	Comparison of control strategies using MATLAB-Simulink.	PMP is presented as the best EMS.
[25]	Energy management of heavy-duty fuel cell vehicles in real-world driving scenarios: Robust design of strategies to maximize the hydrogen economy and system lifetime	Yes	2021	Compare different EMS to optimize durability and consumption for a 300 kW FCS and battery using MATLAB.	Single powertrain architecture study. Sets the basis for the sizing study performed in the present paper. No dynamics change.
[26]	Offline optimal energy management strategies considering high dynamics in batteries and constraints on fuel cell system power rate: From analytical derivation to validation on test bench	Yes	2021	Different dynamics for FCS in the railway sector. Simulations with MATLAB and validated experimental models.	Dynamic control made using the power, using the current density may affect.
[27]	Online adaptive equivalent consumption minimization strategy for fuel cell hybrid electric vehicle considering power sources degradation	Yes	2019	EMS to optimize durability. Uses a battery and supercapacitor to be able to adapt to the desired current density.	The auxiliary elements may not be needed when having two FCS.
[28]	Genetic algorithm based optimal powertrain component sizing and control strategy design for a fuel cell hybrid electric bus	No	2009	Comparison of different powertrain architectures with FCS, battery and ultracapacitors. The authors use MATLAB and ADVISOR to carry out the optimization.	Simple FCV model.
[29]	Fuel cell electrified propulsion systems for long-haul heavy-duty trucks: present and future cost-oriented sizing	Yes	2022	FCV cost study simulating with MATLAB models.	No multi-FCS powertrain. Shows what the existing FCV trends lack.
[30]	Online hierarchical energy management strategy for fuel cell based heavy-duty hybrid power systems aiming at collaborative performance enhancement	Yes	2023	Multi-FCS for heavy-duty using both Dspace and MATLAB-Simulink.	Need of different size FCS combination.
[31]	A Review of Fuel Cell Powertrains for Long-Haul Heavy-Duty Vehicles: Technology, Hydrogen, Energy and Thermal Management Solutions	Yes	2022	Literature review that shows the current trends for FCHDV.	Need of different size FCS combination.

Table 3
Existing literature reviewed, part 3.

Ref.	Title	Recent study (<5 years)	Year	Basic approach and methods	Limitations
[32]	Optimization of Component Sizing for a Fuel Cell-Powered Truck to Minimize Ownership Cost	Yes	2019	Sizing study for TCO analysis using both Autonomie by ANL and MATLAB/Simulink.	Uses predefinied autonomitve software to simulate the vehicles.
[33]	Life cycle environmental and cost comparison of current and future passenger cars under different energy scenarios	Yes	2020	TCO and LCA analyses.	The focus of the paper is on the methodologies implemented rather than the used data.
[34]	The Effect of Fuel Cell and Battery Size on Efficiency and Cell Lifetime for an L7e Fuel Cell Hybrid Vehicle	Yes	2020	Sizing study on efficiency and durability for a FCEV using Simulink.	Example of the many existing passenger car studies, which have different needs than the HD sector.

2.1.1. Vehicle architecture

The vehicle model used is based on the Hyundai XCIENT fuel cell truck [39], the first heavy-duty FCV to be commercialized. The propulsion system integrated into this vehicle comprises two different FCS working in parallel combined with an electric battery. The reason for choosing this architecture for the powertrain comes from the current standardization trend in the FC market. This market trend implies that FCS is intended to be massively produced with a fixed net power output of around 100 kW. Therefore, if any application requires a power higher than 100 kW, a number n of FCS is used instead of an FCS with higher maximum power. In addition, this design of the propulsive system gives a high degree of flexibility in the optimization of the performance and durability of the stacks. General data about the Hyundai XCIENT [39] required to generate the vehicle model can be found in Table 4.

It is important to remark that, during the performed sizing studies, the mass of the vehicle was kept constant with a value of 18 000 kg (normal driving value, Table 4). The reason behind this mass choice is the total maximum power of the multiple FCS, which is kept constant

Table 4
Reference data for the heavy-duty FCV based on the Hyundai XCIENT fuel cell truck [39].

	Dimensions
Wheel base	5.13 m
Length	9.745 m
Width	2.515 m
Height	3.73 m
	Weight
Empty vehicle	9795 kg
Normal driving	18 000 kg
	H_2 tank
Filling pressure	350 bar
Capacity	32.09 kg
	Battery
Technology	NMC Li-ion
Capacity	3 packs of 24.4 kWh (73.2 kWh)
	Other
Transmission	ATM S4500 (Allison)/6 forward speed and 1 reverse speed
Configuration	4 × 2

Table 5
Maximum stack power output of the multiple FCS configurations considered for the sizing of the HDFCV.

	Max. stack power 1 (P_{FC1})	Max. stack power 2 (P_{FC2})
Design 1	120 kW	120 kW
Design 2	140 kW	100 kW
Design 3	160 kW	80 kW

at 240 kW for all the studied cases. Despite the constant power choice, the power distribution of the powertrain has been studied for the three designs shown in Table 5. The reason behind this differential design can be understood by the actual modular trend in the HD sector (1.3). Using a design composed of a set of FCS instead of a large FCS with high power gives additional flexibility during the design phases of the vehicle, which would suppose an important benefit for manufacturers.

The H_2 tank and battery capacity are also kept constant during the studied cases so that the energy content of the vehicle remains the same, thus not affecting the range capacity. The model used for the electric battery is a group of 100 cylindrical cells separated in 25 parallel sets to supply the needed power by the e-motor. Each mentioned cell had a nominal voltage of 3.6 V and a capacity of 3.35 Ah. The carried cargo could be the only value that could influence the weight of the vehicle, but this would not change the architecture of the powertrain. The established mass of 18 000 kg is appropriate for comparison since the manufacturer has stated that this vehicle can achieve a range of 400 km under this mass condition.

2.1.2. Fuel cell system model

Any FCS model requires not only the FC stack but also a set of auxiliary components to operate correctly in driving cycle conditions, i.e., the balance of plant (BoP). The model of the polarization curve establishes the relation between current and voltage, which has significant importance on the behavior of the FC. In this study, this curve is obtained by using the following numerical model:

$$V_{FC} = V_{OC} - V_{act} - V_{ohm} - V_{conc} \tag{1}$$

$$V_{act} = \begin{cases} \frac{R_{gas}T}{2F}\left(\frac{i}{i_0}\right) \\ \frac{R_{gas}T}{2\alpha F}\ln\left(\frac{i}{i_0}\right) \end{cases} \tag{2}$$

$$V_{ohm} = R\,I \tag{3}$$

$$V_{conc} = -C\ln\left(1 - \frac{i}{i_l}\right) \tag{4}$$

In the previous set of equations, V_{OC} represents the voltage of the fuel cell stack under open circuit conditions, whereas V_{act}, V_{ohm}, V_{conc} are the voltage losses that should be taken into account in FCS: activation, ohmic and concentration voltage losses respectively. The estimation of these losses comes from more detailed submodels. In the case of the activation losses, the current exchange density (i_0) value is related to temperature, oxygen partial pressure, electrochemical reaction activation energy, and electrode roughness as stated in [40]. The ohmic resistance mainly controls the calculation of the ohmic losses. This resistance (R) has been obtained considering that the ionic resistance of the membrane changes with its water content [41]. Finally, some of the variables used in the losses calculation are obtained by calibrating the model with experimental data [42,43]; these values are the reference exchange current density, reference ohmic resistance, charge transfer coefficient (α), mass transport loss coefficient (C), limiting current density (i_l), and open circuit voltage losses. This calibration was carried out using the genetic algorithm toolbox provided by GT-Suite. Furthermore, this calibration process considers experimental data at different temperature and pressure conditions so that the FC behavior is closer to the actual driving cycle conditions. The presented model Eqs. (1)–(4), the calibrated GT-suite data and the established ambient conditions can be used to obtain polarization curve results that can be compared with the experimental ones. Fig. 2 shows that the modeled fuel cell reproduces the behavior observed in the experimental case with an error not more significant than a 2%. The model validation explanation is further explained by a previous study [44].

The validated FC stack was integrated into a BoP model (Fig. 3) composed of four main circuits: anode, cathode, cooling and electric. The designed model had already been optimized in a previous study [36].

The anode or hydrogen circuit connects the H_2 tank to the stack. A valve that regulates the anode pressure controls the flow of H_2 into the system. The flow into the stack is controlled by an active recirculation loop which inputs the excess H_2 at the FC stack outlet with a pump that is also used to control anode stoichiometry. The cathode or air circuit includes an electric centrifugal compressor used to increase the air pressure as in the anode side; this compressor is also used to control the mass flow of air coming into the system. After the compressor, a heat exchanger is used to cool down the fluid, and a humidifier is integrated to increase RH, thus reducing the ohmic losses in the stack. The cathode output is connected to the humidifier so that the water vapor can be used to increase the water content of the air at the inlet of the cathode. The output of the cathode also controls its pressure by regulating the size of the outlet valve. This BoP model considers the power consumption of each of its components to obtain a precise net power of the FCS. In addition, the control of each BoP component is performed by a PID controller following the optimum operation that ensures maximum FCS net efficiency.

2.2. Energy management strategy

The energy management strategy (EMS) allows the control of the power split in any propulsive system. Three different power sources can be distinguished in the studied vehicle architecture: two FCS and a battery. Therefore, the purpose of the EMS is to find the power distribution that can optimize the performance of the powertrain while minimizing a specific cost function [45]. If the EMS provided an incorrect power distribution, the sizing study would be biased, and its results would not correspond with the desired optimization. The Optimal Control (OC) strategy provides the optimal energy split for each powertrain evaluated. This design makes this strategy particularly appropriate for these tests; each scenario of the sizing study is carried

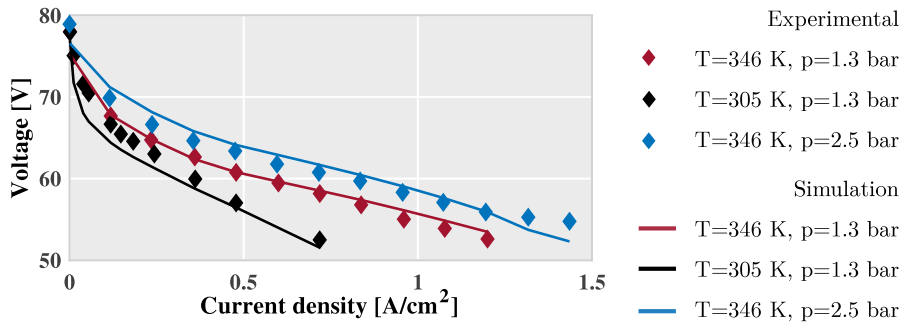

Fig. 2. FC model validation results at different temperatures and pressures. Experimental data retrieved from [42,43].

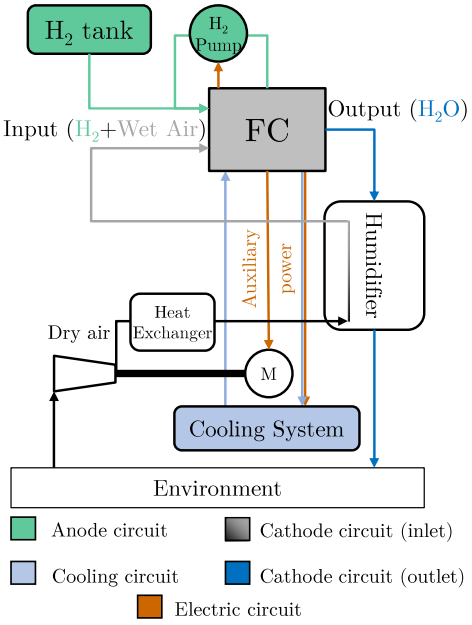

Fig. 3. FC system outline composed by the FC stack and the BoP components developed initially and optimized at [36].

out in optimal energy split conditions. Therefore, in the present study, the performance obtained for each design is optimum for that particular design, thus making the benchmark fair [46].

It is well-known that in an FCV as the studied truck, the power demanded by the driving cycle can come from any of the existing propulsive system (Eq. (5)).

$$P_{dem} = P_{bat} + P_{FC} \tag{5}$$

The cost function to be minimized in this study is the H_2 consumption. Therefore, the control parameter is the power of the two fuel cell systems ($P_{FC}(u)$). The variable u on which these values depend is, in this case, the current density. In addition, the state-of-charge of the battery along the studied driving cycles follows the charge-sustaining mode, which means that during the whole process, the charge state of the battery at the beginning and the end of the cycle is the same (Eq. (7)). Minimizing the control parameter along the duration of the driving cycles means minimizing the power consumed in the form of H_2 (P_f). The variable to be minimized is J, which represents the sum of the consumed H_2 along the time domain (t_0, t_f), and it can be shown as follows (6).

$$J = \int_{t_0}^{t_f} P_f(u(t), t)\, \mathrm{d}t \tag{6}$$

Considering that P_b represents the battery power consumption and E_b the battery energy content, the SOC sustenance condition is stated in the equation below.

$$\int_{t_0}^{t_f} P_b(u(t), E_b(t), t)\, \mathrm{d}t = 0 \tag{7}$$

Following Pontryagin's Minimum Principle (PMP), a global optimization problem can be solved as a set of local optimization problems. Therefore, being H the Hamiltonian function:

$$H = P_f - \lambda \dot{E}_b = P_f(u(t), t) + \lambda P_b\left(u(t), E_b(t), t\right) \tag{8}$$

If u* and E_b^* are the optimized control variable and energy content of the battery, it can be stated that:

$$H\left(u^*, E_b^*, \lambda^*, t\right) \leq H\left(u, E_b^*, \lambda^*, t\right) \forall u \in U, t \in [t_0, t_f] \tag{9}$$

It must be taken into consideration that P_f and P_b have the same units, therefore, λ is dimensionless. PMP relates this parameter with the energy content of the battery (Eq. (10)). Introducing also the power produced by the battery (P_{batt}):

$$\dot{\lambda} = \frac{\partial H}{\partial E_b} = \lambda \frac{P_b}{E_b} = \lambda P_{batt} \frac{\partial\left(P_b / P_{batt}\right)}{\partial E_b} \tag{10}$$

Considering $\left(P_b / P_{batt}\right)$ represents the battery efficiency and since the open circuit voltage and ohmic resistance (battery parameters) are slightly dependent on the energy contained in the battery or state-of-charge (SOC), λ can be established as a constant. With this previous statement in mind, it can be noted that optimizing H_2 consumption implies varying the value of λ while the charge sustaining condition (Eq. (7)) is fulfilled and to minimize function H (Eq. (8)) in each time step.

The EMS can include restrictions depending on the application of the vehicle. The studied heavy-duty vehicle uses two different FCS; therefore, dynamic restrictions ($|\mathrm{d}i/\mathrm{d}t|$) are imposed in both of them. The Hamiltonian changes accordingly and is presented in (Eq. (11)).

$$H = P_f - \lambda \dot{E}_b + L_1 + L_2 \tag{11}$$

L_1 and L_2 now represent the limiting functions. These functions would take the value of the Hamiltonian to infinite if the operation exceeded the established restrictions (Eqs. (12) and (13)). These restrictive parameters (L1 and L2) reduce the decision space. Thus, it could seem that finding the optimal value could be faster and would imply a lower computational cost. Nevertheless, limiting the dynamics makes the FCS deviate from its optimal point regarding the established parameter, H_2 consumption. This will be later shown in the results (Sections 3 and 4), as H_2 consumption increases when dynamics get lower. In addition, the current density space that the EMS uses to optimize the FCS operation is discretized in an adaptative way, i.e., it always considers a high number of points within the current density limits that comply with the imposed limitations.

$$L1 = \begin{cases} 0 & |\mathrm{d}u_1/\mathrm{d}t|\,(t+\mathrm{d}t) \leq |\mathrm{d}i/\mathrm{d}t|_{max_1} \\ \infty & |\mathrm{d}u_1/\mathrm{d}t|\,(t+\mathrm{d}t) > |\mathrm{d}i/\mathrm{d}t|_{max_1} \end{cases} \tag{12}$$

$$L2 = \begin{cases} 0 & |\mathrm{d}u_2/\mathrm{d}t|\,(t+\mathrm{d}t) \leq |\mathrm{d}i/\mathrm{d}t|_{max_2} \\ \infty & |\mathrm{d}u_2/\mathrm{d}t|\,(t+\mathrm{d}t) > |\mathrm{d}i/\mathrm{d}t|_{max_2} \end{cases} \tag{13}$$

Table 6
Reference degradation rates (1st layer) to be scaled.

Condition	δ [fraction V loss]
Low power [/h] $\left(\left.\frac{d\delta}{dt}\right\|_{lp,ref}\right)$	$1.26 \cdot 10^{-5}$
Load change [/cycle] $\left(\left.\frac{d\delta}{dn_{lc}}\right\|_{ref}\right)$	$4.94 \cdot 10^{-7}$
High power [/h] $\left(\left.\frac{d\delta}{dt}\right\|_{hp,ref}\right)$	$1.03 \cdot 10^{-5}$
Start-stop [/cycle] $\left(\left.\frac{d\delta}{dn_{ss}}\right\|_{ref}\right)$	$1.95 \cdot 10^{-5}$

Therefore, the EMS has two control variables, the current densities of each FCS (u_1 and u_2). The decision spaces for both of them can be represented in the following matrices:

$$u_1 = \begin{bmatrix} u_{11} & u_{12} & \cdots & u_{1n} \\ u_{11} & \ddots & & \vdots \\ \vdots & & \ddots & \vdots \\ u_{11} & \cdots & \cdots & u_{1n} \end{bmatrix} \tag{14}$$

$$u_2 = \begin{bmatrix} u_{21} & u_{21} & \cdots & u_{21} \\ u_{22} & \ddots & & \vdots \\ \vdots & & \ddots & \vdots \\ u_{2n} & \cdots & \cdots & u_{2n} \end{bmatrix} \tag{15}$$

Therefore, the Hamiltonian turns into a matrix. Selecting the position of the minimum value in H allows us to obtain the values of u_1 and u_2 that minimize the H_2 consumption.

2.3. Degradation model

The durability of an FC represents a significant parameter when designing any FCS. The level of degradation influences the performance in such a way that it determines its durability. The main objective of a degradation model is to predict in a precise and quantitative way the degradation rate of the FC. This kind of model is mainly affected by the EMS and the conditions in which the system operates. Managing the power produced is essential because low-load or high-load conditions trigger electrochemical mechanisms that, together with high load-changes, are a vital degradation source. The chemical nature of the degradation process also depends on the temperature and humidity conditions.

The semi-empirical degradation model used in this study considers all the previously mentioned phenomena. These mechanisms are considered using degradation rate coefficients obtained experimentally [47] for known conditions (i, T, and RH). In addition, this data was later adjusted for validation purposes (Table 6). The used model was developed in previous studies and can be found in more detail in [37].

The degradation process produces a variation in the voltage produced by the stack. This voltage drop provides a good way to measure degradation. Therefore, the degraded ratio (δ) can be obtained by the following expression (Eq. (16)):

$$\delta = 1 - \frac{V_{deg}}{V_{FC}} \tag{16}$$

this FC degradation model aims to predict the voltage loss ratio based on the FC operating conditions and electrochemical phenomena. For this purpose, how δ changes along time are computed by using the known reference degradation rates (Table 6). The modeled expression is stated as follows (Eq. (17)):

$$\delta = \int_0^t \left[\left.\frac{d\delta}{dt}\right|_{lp} + \left.\frac{d\delta}{dt}\right|_{lc} + \left.\frac{d\delta}{dt}\right|_{hp} + \left.\frac{d\delta}{dt}\right|_{nt} \right] dt + \frac{d\delta_{ss}}{dn_{ss}} n_{ss} \tag{17}$$

This expression defines how the voltage loss ratio changes depending on how the FC is operated. The different degradation sources are classified as low-power (lp), load-change (lc), high-power (hp), natural or medium-power (nt), and start-stop (ss). The degradation rate coming from each one of these sources is scaled accordingly with the electrochemical phenomena and the operating conditions. This can be better explained by expanding the previous expression (Eq. (17)) into the set of equations presented below (Eqs. (18)–(22)).

$$\left.\frac{d\delta}{dt}\right|_{lp} = \left.\frac{d\delta}{dt}\right|_{lp,ref} \cdot \xi_{lp}(i) \cdot \tau(T) \cdot \eta\left(\overline{RH}\right) \tag{18}$$

$$\left.\frac{d\delta}{dt}\right|_{lc} = \left.\frac{d\delta}{dt}\right|_{lc,ref} \cdot \xi_{lc}(i) \cdot \tau(T) \cdot \eta\left(\overline{RH}\right) \tag{19}$$

$$\left.\frac{d\delta}{dt}\right|_{hp} = \left.\frac{d\delta}{dt}\right|_{hp,ref} \cdot \xi_{hp}(i) \cdot \tau(T) \cdot \eta\left(\overline{RH}\right) \tag{20}$$

$$\left.\frac{d\delta}{dt}\right|_{nt} = \frac{\left.\frac{d\delta}{dt}\right|_{hp,ref} \xi_{hp}\left(i_{hp}\right) - \left.\frac{d\delta}{dt}\right|_{lp,ref} \xi_{lp}\left(i_{lp}\right)}{i_{hp} - i_{lp}} \left(i - i_{lp}\right) + \left.\frac{d\delta}{dt}\right|_{lp,ref} \xi_{lp}\left(i_p\right) \tag{21}$$

$$\frac{d\delta_{ss}}{dn_{ss}} = \left.\frac{d\delta}{n_{ss}}\right|_{ref} \tag{22}$$

The electrochemical phenomena in the FC is modeled by the scaling function ξ, which depends on the current density and increases or decreases the degradation according to the behavior of its value. In addition, some limits have been established for current degradation: i_hp and i_{lp} are the maximum and minimum values for which high and lower degradation are considered. These have been calibrated to 1 and 0.33 A/cm^2 from experimental data [47]. Finally, the degradation rates are scaled with the operating conditions through τ and η, which depend on T and $\overline{RH}$ (temperature of the stack and relative humidity as an average between anode and cathode values).

The representation of the electrochemical phenomena in the FC in the degradation model (Eqs. (18)–(22)) is not trivial and should be explained in further detail.

When working at low power or idle condition, the degradation of the FC is controlled by ξ_{lp}. The worsening of the FC stack performance under these conditions was observed experimentally by a change in the fluoride release rate (FRR) [48] and by the catalyst surface carbon corrosion, which affects the anodic peak current [49]. Then, this function has been modeled (Eq. (23)) so that it is one at 0.01 A/cm^2, the value in which the degradation rates were measured.

$$\xi_{lp} = -0.176 \cdot \ln i + 0.169 \tag{23}$$

ξ_{hp} or high power degradation has a much more intuitive behavior. In these high-load scenarios, degradation comes from the high temperatures produced in the stack. These temperatures come from the currents, which allow the function to be modeled as in Eq. (24).

$$\xi_{hp} = \frac{i}{i_{hp}} \tag{24}$$

As it is known, high-dynamic conditions also influence degradation (ξ_{lc}). Load-change degradation rate depends on the rate at which the current density is changed, which is related to both the driving cycle and the EMS (di/dt). The reference value for ξ_{lc} was obtained for a known current step $|\Delta i|_{ref}$. Obtaining a value adaptable for every time and current step would require a new definition of ξ_{lc}. Considering the increase and decrease current step, the modeled equation is shown in Eq. (25).

$$\xi_{lc}\left(\frac{di}{dt}\right) = \frac{|\Delta i|_{dt}}{2\,|\Delta i|_{ref}} \tag{25}$$

At medium-load driving conditions degradation is modeled by considering the continuity of ξ_{lp} and ξ_{hp}. However, in this range of powers, most degradation mechanisms are not present, and degradation happens due to natural voltage decay of the FC stack; that is the reason why this kind of degradation is called natural degradation.

Degradation generated by the operating conditions of the working FC are also significant. There exists a high relationship between temperature and degradation due to the chemical nature of this process. The

experimental results in [47] shows the relation between the fluoride release rate change and temperature. In addition, it has been proven [50] that temperature increases platinum (Pt) dissolution mechanisms which causes electrochemical surface area (ECSA) decrease rate. These relations and the collected experimental data allow the modeled expression in Eq. (26).

$$\tau(T) = -5.390 \cdot 10^{-4} T^2 + 0.399 \cdot T - 71.576 \quad \forall T \in [310, 373.15] \tag{26}$$

Function η measures how RH increases degradation by ECSA decrease rate (Pt grain growth). This degradation phenomenon takes RH as a mean value between anode and cathode, and it has been modeled considering the experimental data from [51] (voltage cycling degradation tests).

$$\eta(RH) = 0.10646 \exp^{0.028 \cdot RH[\%]} \tag{27}$$

Finally, the validation of the model was carried out in previous studies [37,38] by performing a simulation of an FC city bus stack that operates in real driving cycle conditions of one of its usual daily routes [47]. Then, the obtained results were compared with the experimental ones, and the predicted degradation showed an error lower than 0.1%.

2.4. Driving modes

The main focus of the performed study is to analyze H_2 consumption and durability of different sizing distributions of the FC powertrain. The heavy-duty nature of the studied vehicle makes HDDT an appropriate driving cycle for the simulations. The procedure that has been carried out can be divided into two different parts.

At first, an equal power architecture is studied (Section 3). In this analysis, 2 FCS of the same power, 120 kW, are simulated for different dynamic restrictions (0.1, 0.001, and 0.001 A/cm^2 s) to understand the behavior of consumption and degradation for different current controls. Then, for the second part of the study (Section 4), the previously stated differential control models are combined with the different proposed FCS sizings (Table 5).

The differential control used in each of the cases represents an important novelty respect to other literature works, as it has been stated in Section 1. A different control of the current density, allows faster or slower responses by the FCS when power is demanded by the imposed driving conditions. The speed of the reaction response influences the power the FCS is able to reach at each moment and, therefore, the power the battery needs to supply to meet the demand. The differential control imposed represent a restriction in the performance of the FCS that will be considered by the EMS when obtaining the desired current. This restriction allows the EMS to take faster decisions, but depending on the chosen dynamics, there will be different consequences in the powertrain performance. This has not been explored in the recent literature, thus implying a knowledge gap.

This set of combined cases allows an understanding of the effect of different size distributions and the differential dynamics on heavy-duty vehicle performance and FC durability.

3. Differential control applied to multi-FCS

3.1. Effect on the current density evolution

The analysis of the dynamics-limited EMS is done for the equal-power FCS design (120 kW) with the HDDT driving cycle, which implies a medium-to-high power operation. The limits on the dynamics that have been established for the present analysis are a minimum $|di/dt|$ of 0.001 A/cm^2 s and a maximum of 0.1 A/cm^2 s.

First, one of the fuel cell systems (FCS_1) is maintained under the maximum current density rate of change (0.1 A/cm^2 s). In contrast, the current density dynamics of the second are changed (Fig. 4 A, B and C). These graphs show how when the dynamic is higher, the EMS selects the current density that adapts to the demanded power at each instant. Thus, Fig. 4A shows how the current density can rapidly adapt to the required power. In Fig. 4B, as one current density gets more restrictive, one of the FCS is not able to adapt in such a fast way. In this case, the high dynamics FCS adds the required power at the dynamic peaks. In 4C, the FCS with low dynamics produces an almost constant current density. The active FCS reacts to fulfill the required demanded current.

Note that the powertrain control strategy for the simulated cases was designed to minimize the H_2 consumption, given a limitation in the FCS dynamics, as explained in Section 2.2. In this case, one of the expected disadvantages of FCS_1 is that it should be highly influenced by load-change degradation.

Then, the current density rate of FCS_1 is changed to 0.01 A/cm^2 s. At the same time, the second remains variable (Fig. 4D and E), and then both FCS are operated under the lowest selected dynamics (Fig. 4F). This current density change represents a design in which the FC stack durability should be improved compared to the previous one (Fig. 4A, B and C). In none of the combinations presented in Fig. 4D, E and F, the dynamics experienced by the FCS are as high as in the previous tests (Fig. 4A, B and C), which implies lower degradation.

Fig. 4 shows the whole set of possible current density rates used in the performed tests. These figures present how the recent density changes to keep the state-of-charge (SOC) constant at all times and adapt to the demanded power, as explained in Section 2.2 when working under different levels of dynamics but in the same driving cycle.

From the comparison of 4A and F, it is interesting to see how much different current density evolutions can fulfill the requirements of the cycle. This is possible due to the presence of the electric battery in the powertrain system, which allows the coverage of the power peaks in which the low dynamics FCS cannot supply the needed current density.

Fig. 4A, D, and F show an equal current density variation strategy. The EMS chooses the same current distribution for the driving cycle conditions in these three simulations. Thus, the double FCS powertrain works as a unique FCS to achieve the minimum H_2 consumption. Besides, simulations in Fig. 4B, C, and E, one of the FCS has higher dynamics, so it is expected to be more affected by load-change degradation, while the other acts as the primary and stable source of power, as it happens in a usual range-extender configuration.

In Fig. 4B and C, when the current density change over time of FCS_1 is restricted to 0.1 A/cm^2 s, the oscillations of the current density values of this FCS increase. In the case of 4B, when there is a low power demand, FCS_2 cannot decrease the current in the required time. Therefore, FCS_1 reduces its power contribution to adjust the power needed. In case of high power demand, due to the stable current density values produced by FCS_2, the SOC is high enough to cover part of the peak power and reduce the maximum current density needed from FCS_1. However, simulation 4C differs in the power peaks. In the first part of the driving cycle, the power produced by FCS_2 is so low that it cannot generate a high battery SOC that could be used when the e-motor power demand is high. Consequently, the current density produced by FCS_1 has large oscillations and higher current density peaks during the driving cycle operation and, therefore, higher degradation.

3.2. Effect on durability and performance

The obtained results for performance and durability of the studied cases are presented in Figs. 5 and 6, respectively. The quality of the combined FCS performance is measured by its ability to minimize H_2 consumption.

The distance the vehicle can travel with each of the simulated configurations represents the durability of the FCS propulsive system. Following the DoE criteria [52], the end of life of the FCS is established

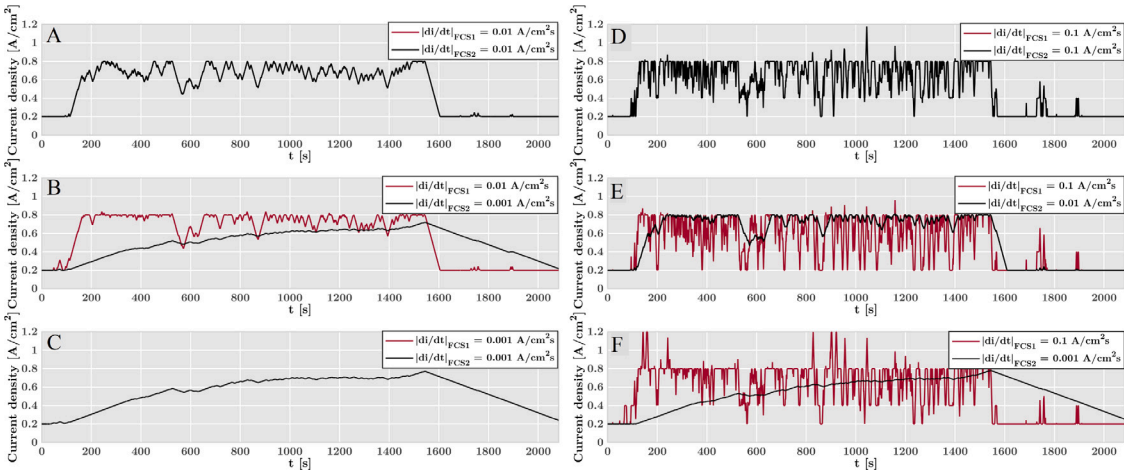

Fig. 4. Evolution of the current density for the FCS_1 and FCS_2 (120 kW both) along the HDDT driving cycle with differential control dynamics ranging from 0.1 to 0.001 A/cm^2 s.

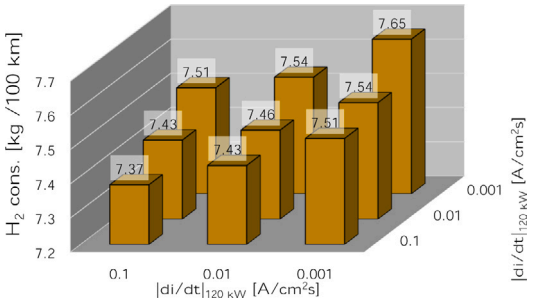

Fig. 5. H_2 consumption of the different dynamic limitations considered for the powertrain composed of two 120 kW FCS.

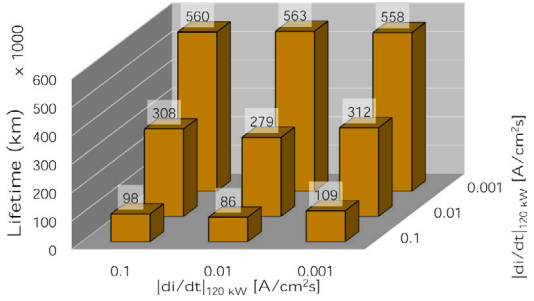

Fig. 6. Durability of the different dynamic limitations considered for the powertrain composed of two 120 kW FCS.

when its voltage drops by 10% at a current density of 1 A/cm^2. However, Fig. 6 only shows the durability of one of the FCS, corresponding to the right axes $\left|\frac{di}{dt}\right|$ values. Since the size of both FCS is the same, the durability results for the other FCS are symmetrical to those presented in this figure. Thus, they are omitted to improve readability.

The previous graph leads to the understanding that the change in dynamics highly influences the durability of an FCS. A good practice would be to change the dynamics of the FCS depending on the driving mode of the vehicle. Therefore, lower dynamics would be used at the beginning stages, with a higher degradation level. This would allow a more progressive degradation of the FCS.

Fig. 5 clearly shows the effect that different levels of dynamics have on H_2 consumption. High dynamics applied on both FCS (0.1 A/cm^2 s) imply a consumption of 7.37 kg of H_2 every 100 km, whereas for low dynamics (0.001 A/cm^2 s) this value rises to 7.65 kg H_2/100 km. The consumption difference between the most dynamically-different cases is not very high; it just supposes a 3.8% saving of H_2 in the best scenario. In previous studies for light-duty applications [37], a current density rate of change reduction implied a much higher H_2 consumption saving (up to 8%). However, this is due to the more stable nature of the HDDT driving cycle compared to WLTC 3b. Therefore, imposing lower dynamics for heavy-duty FCV may bring more benefits than for the passenger car application.

In contrast, the durability plot (Fig. 6) shows a significant difference between high and low dynamics. When both FCS operates under low dynamics, the lifetime of the vehicle is 558 000 km, whereas, when dynamics are high, its durability is reduced to 98 000 km. Therefore, the variation in the current density rate of change from the highest to lowest dynamics tested produces a 471% increase in the durability of the FC stack. Since the flows involved in the FCS, coolant, anode, and cathode flows, are proportional to the current density, lowering the dynamics of the current allows an easier stabilization of these flows. Thus, having more stable flows reduces the danger of starvation, flooding, or harmful phenomena for the aging of the FC stack. Therefore, the trade-off between performance and durability obtained from these simulations imply that when having different current density rates of change for each FCS ($FCS_{1=0.001}$ A/cm^2 s, FCS_2 = 0.1 A/cm^2 s), the H_2 consumption increases only a 3.8%. At the same time, there is a lifespan increase of 471%. Consequently, the influence on performance and durability is very different for the same dynamic variation.

In addition, the effect of current density variations on durability is important for each FCS. Fig. 6 shows that when FCS_1 works under high dynamics (0.1 A/cm^2 s), its durability is low. However, the lifespan of FCS_1 is not constant for different dynamics imposed on FCS_2. When the current density variation of FCS_2 is limited to 0.01 A/cm^2 s (Fig. 4B), the load-changes experienced by FCS_1 are higher to reach the power demand that FCS_2 cannot reach. Thus, there is a durability decrease of 11.58% (86 000 km). If the current rate decreases even more to 0.001 A/cm^2 s, the EMS provides energy to the battery when the power supply is under demand and then uses this battery power to cover the power peaks. Therefore, the FCS durability increases to 109 000 km (11.60% increase). This durability variation is insignificant when dynamics are low, as Fig. 6 shows; the difference in these cases is smaller than 1%. Therefore, Fig. 6 shows that when one of the FCS works under high dynamics, it is essential to select the appropriate current density rate change for the other FCS because the use of high dynamic levels would lead to lower durabilities.

The importance of differential control of the current density variation depends on the application and purpose of the system. Using a moderate dynamic for both FCS (0.01 A/cm^2 s) is very beneficial compared to a combination of high and moderate dynamics (0.1 A/cm^2 s and 0.01 A/cm^2 s), it produces an increase of almost three times of the

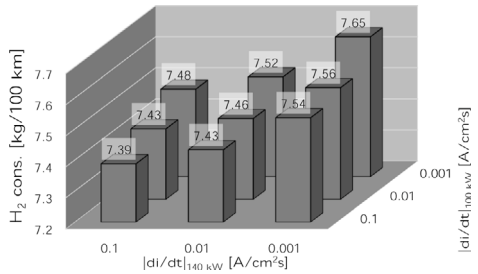

Fig. 7. H_2 consumption of the different dynamic limitations considered for the powertrain composed of a 100 kW and a 140 kW FCS (design 2).

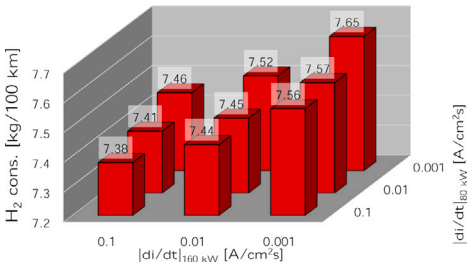

Fig. 8. H_2 consumption of the different dynamic limitations considered for the powertrain composed of an 80 kW and a 160 kW FCS (design 3).

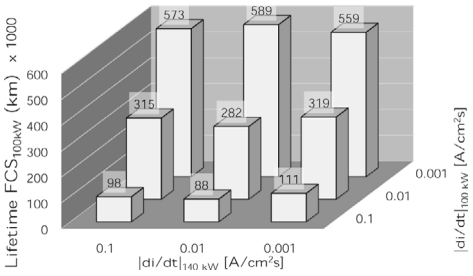

Fig. 9. Durability of the 100 kW FC stack with different dynamics limitations considered for the powertrain composed of a 100 kW and a 140 kW FCS (design 2).

lifetime of the FC stack with just a 0.4% increase in H_2 consumption. However, low dynamics (0.001 A/cm^2 s) produce an increase of 1.5% of H_2 consumption in exchange of a 79% increase in durability, when compared to a combination of moderate and low dynamics (0.01 A/cm^2 s and 0.001 A/cm^2 s). This benefit is less important than in the case of the previous dynamic. Therefore, the importance of using differential control (Fig. 4) depends on the combination of emissions and cost of H_2 and FCS production.

4. Differential control and sizing design strategies

4.1. Dynamics-limited energy management strategy and FCS sizing crossed-analysis

Differential control of the current density variation is an excellent way to improve the durability or performance of an FCS powertrain. This strategy allows using one FCS as a more stable power source while the other is used to supply the power demanded by the driving cycle during its high load peaks. Combining this energy distribution with a differential FCS sizing may benefit the propulsive system. This configuration may allow improving durability features for the bigger FCS, which is more expensive and produces a higher environmental impact. The present analysis studies the designs presented in Table 5 also changing the current density variation in time from 0.1 A/cm^2 s to 0.001 A/cm^2 s.

4.2. Effect on durability and performance

The main objective of this study is to understand the influence of differential control and sizing (Table 5) on performance and durability. The analyzed sizing designs (Table 5) represent different cases that could be used in real heavy-duty fuel cell vehicles following the actual modular trend in this sector. The first design (equal power FCS) has already been studied in detail in Section 3. Figs. 7 and 8 show the H_2 consumption for designs 2 and 3 when varying the current density rate of change of each FCS.

In Figs. 5, 7 and 8, the H_2 consumption difference in the equal current change values is lower than 0.3%. Thus, when the dynamics are the same for both FCS, the system behaves as if there was only one FCS with a total power of 240 kW. In conclusion, differential sizing supposes no benefits if no differential current change control exists.

When the difference in power of the two FCS is more significant (160 kW and 80 kW), the H_2 consumption is more minor for high values of the current density change rate (0.1 A/cm^2 s) in the bigger FCS (160 kW). When the high-power FCS has lower dynamics (0.001 A/cm^2 s), the consumption is lower for the case in which there is a smaller difference between the FCS powers (140 kW and 100 kW). It had already been seen in Fig. 5 that low consumptions come from high dynamics. Therefore, it is reasonable that the higher power multi-FCS gives the best behavior in terms of consumption because less H_2 and current are needed to reach the power peaks.

In any case, it is essential to remark that the variation between the H_2 consumptions between the different designs with the same dynamics is never greater than 0.7%. Thus, from the performance point of view, the FCS size is not a limiting parameter and has a negligible impact if the total maximum power provided by both FCS remains constant. However, the study of the dynamics for different designs shows that the effect of limiting the current density rate of change is significant for the performance of the system. In the 80 kW and 160 kW cases, the consumption varies by 1.3% (7.46 to 7.56 kg of H_2/100 km) for the different dynamic combinations.

The durability analysis is slightly different from the performance one. This property depends on the particular FC stack. Thus, it is studied for each FCS separately. Figs. 9–12 show the obtained durability results for the different tested dynamics.

The durability plots show a similar trend as in Fig. 6. The durability of the stack depends mainly on its current change rate, but it also has minor variations depending on the current change over time of the other FCS. When the dynamics of the non-observed FCS change, the evolution of the current density controlled by the EMS optimizer changes, and degradation due to load changes affect the FCS differently. The observed trend is the same as in the equal-power design (design 1). When the 140 kW FCS works under high dynamics, its lifetime depending on the 100 kW dynamics can change up to 17.5%, whereas when it works under low dynamics, it would only change a 0.3%. Design 3 shows the same effect of dynamics on durability. When the 160 kW has a current density rate of change of 0.1A/cm^2 s, for different dynamics of the small FCS, its lifetime can change up to a 14.3%, whereas in the case of the low dynamic, the difference would be much smaller (1.9%). In addition, the effect of the significant FCS dynamics on the small one is the same. The 100 kW FCS lifespan when working with high dynamics shows a variability that can get to 26.1%, in contrast to the low dynamics value of a 5%.

A deep analysis of the obtained data would need LCA and TCO studies to understand the differences in emissions and costs of the different power distributions of the propulsive systems. However, it is possible to compute a simplified estimation of how the different structures would affect the powertrain choice. This simplified calculation

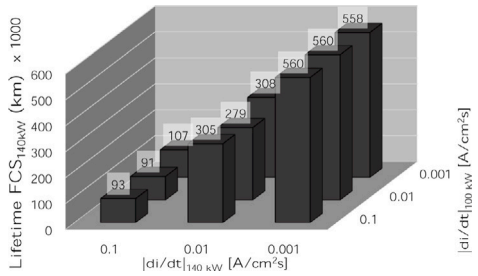

Fig. 10. Durability of the 140 kW FC stack with different dynamics limitations considered for the powertrain composed of a 100 kW and a 140 kW FCS (design 2).

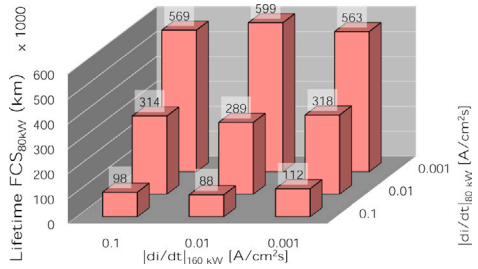

Fig. 11. Durability of the 80 kW FC stack with different dynamics limitations considered for the powertrain composed of an 80 kW and a 160 kW FCS (design 3).

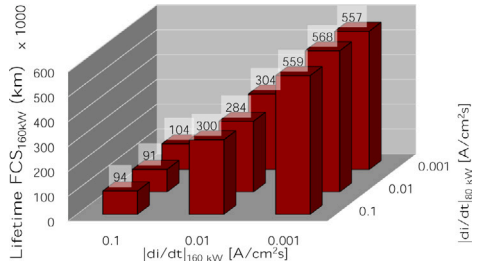

Fig. 12. Durability of the 160 kW FC stack with different dynamics limitations considered for the powertrain composed of an 80 kW and a 160 kW FCS (design 3).

is intended to highlight the potential of differential control and sizing design strategies.

Finally, Fig. 13 is presented to summarize all the obtained results for the different architectures and dynamics tested. This image shows two conditional tables, one showing the H_2 consumption, and other with the durability results. The main purpose of this figure is to give an overview of which of the obtained designs are better for the operation of the FC truck. The conditional format eases the fast understanding of the results. These tables are convenient for fast and general conclusions. It can be noted that fast dynamics decrease the durability of the FCS and low dynamics decrease H_2 consumption. Nevertheless, for further details and comparisons between configurations and dynamics it can be more convenient to analyze the previously presented (Figs. 5 to 12).

A heavy-duty vehicle whose lifetime is 1 000 000 km with a powertrain of equal power FCS (120 kW), one FCS working under high dynamics (0.1 A/cm^2 s) and the other under low dynamics (0.001 A/cm^2 s), is chosen as an example. In this case, to cover the required durability, the vehicle needs 11 FCS that work under 0.1 A/cm^2 s and 2 to work under 0.001 A/cm^2 s (Fig. 6). Considering the cost of a 120 kW FCS to be X, then the cost of the system would be:

$$11 \cdot X + 2 \cdot X = 13 \cdot X \tag{28}$$

This case can be compared with the 80 + 160 kW system. In this scenario, the smaller FCS is operated under high dynamics, and the bigger one works under low dynamics conditions. Applying the same lifetime, this vehicle would need 11 small FCS and two big FCS again. Assuming that the cost of the FCS changes linearly with the maximum output power, the cost of each FCS would be 80/120· X and 160/120 · X. The reader should note that this simplification is purposely made inaccurate since the aim for showing it, is to identify a trend and no data about PEMFC systems greater than 120 kW can be found in the literature. Then, the cost would be:

$$11 \cdot 80/120 \cdot X + 2 \cdot 160/120 \cdot X = 10 \cdot X \tag{29}$$

This calculation is very simplified, but it shows an improvement in the cost of the system. When comparing H_2 consumption (Figs. 5 and 8) the 80 + 160 kW system shows a worse performance (0.7% greater consumption). The cost reduction of 23% is more significant than the slight increase in consumption. Nonetheless, depending on the H_2 price, this 0.7% increase in consumption may outweigh the decrease in production and maintenance costs. For such a reason, since these kinds of studies are out of the scope of this paper, a detailed analysis of the cost and emissions of these vehicles is proposed as future work.

5. Conclusion

The present study has successfully generated results for different FCS-based propulsion systems, considering the strategy of differential sizing and control dynamics. The level of detail of the platform used to create the results gives them a privileged position concerning other analyses from the literature. Combining a detailed degradation model with a full FCV and an EMS capable of choosing the least H_2 consumption option offers an appropriate representation of an actual vehicle.

The obtained data shows the performance of both FCS (measured by its H_2 consumption) and their durability. The combination of different FCS power combinations in the same powertrain represents an important novelty that has not been studied in the existing literature and should be remarked on due to its high value for the HD manufacturing sector. It is also important to note that similar studies for passenger car applications would not be helpful when understanding HD performance because of the different cycle dynamics, power, and weight requirements.

In addition, combining the sizing variations with different control strategies represents a new concept in the current research scenario that should be paid attention to. The different current density rates used have shown a very different FCS performance in terms of consumption and durability, but also depending on the size of the FCS. Thus, the modular trend in FCV manufacturing should also consider the dynamic performance of the system rather than just power and weight.

The conclusions from the performed analyses are important for the future heavy-duty industry design phases because knowing the sizing of the different FCS that optimize performance and durability may help arrange the truck's cargo capabilities and fuel tank size, thus accelerating the deployment of FC technology in the heavy-duty transportation sector.

The analysis of the results leads to the obtention of the following conclusions:

- Increasing the dynamics of the FCS has a beneficial effect on the powertrain performance. The lowest dynamic proposed (0.001 A/cm^2 s) comes together with a 3.8% increase of H_2 consumption. In addition, the different power comparison shows that sizing does not provide an important difference in H_2 consumption (less than a 1%) when the dynamic limitations are equal. These analyses also show that when using two different sizes for each FCS, in terms of performance, it is more beneficial to use the high-power system under higher dynamics than the small one. The large FCS provides most of the system's power, so when it works under high dynamics conditions, the consumption of the system is improved.

		Durability FCS1 [km x 1000]			Durability FCS2 [km x 1000]			H_2 consumption [kg/ 100 km]		
	$\lvert di/dt\rvert_{FCS2}$ / $\lvert di/dt\rvert_{FCS1}$	0,1	0,01	0,001	0,1	0,01	0,001	0,1	0,01	0,001
Design 1 (FCS1 = 120 kW; FCS2 = 120 kW)	0,1	98	86	109	98	308	560	7,37	7,43	7,51
	0,01	308	279	312	86	279	563	7,43	7,46	7,54
	0,001	560	563	558	109	312	558	7,51	7,54	7,65
Design 2 (FCS1 = 100 kW; FCS2 = 140 kW)	0,1	98	88	111	93	305	560	7,39	7,43	7,54
	0,01	315	282	319	91	279	560	7,43	7,46	7,56
	0,001	573	589	559	107	308	558	7,48	7,52	7,65
Design 3 (FCS1 = 80 kW; FCS2 = 160 kW)	0,1	98	88	112	94	300	559	7,38	7,44	7,56
	0,01	314	289	318	91	284	568	7,41	7,45	7,57
	0,001	569	599	563	104	304	557	7,46	7,52	7,65

Fig. 13. Conditional tables of the obtained results.

- The equal power (120 kW) case shows a 471% increase in durability when changing the dynamic limitation from 0.1 A/cm^2s to 0.001 A/cm^2s, which means low dynamics are beneficial for the FCS lifetime. From the different size configurations, it is clear that the higher the power, the higher the effect of dynamics on durability. However, increasing the power is not the only quality that could worsen the durability of the FCS under high dynamics. A small difference between the powers of the FCS is also negative for the high FCS durability because the high-power FCS is used more, degrading faster. This is why the 160–80 kW case shows higher durability for its big FCS than the 140–100 kW case.
- The comparison between performance and durability shows that the improvement of the second can be considered significant compared to the consumption worsening when having lower dynamic behaviors.
- The identification of the optimum design among those considered when applying the differential control and sizing design methodologies depends on the total cost (TCO) and the emissions (LCA) of each different system. The rough example that uses an established value X, which stands for cost or emissions, estimates the difference in results for each sizing coupling. This example (29) shows how a 23% of the manufacturing cost or emissions could be saved if the differential sizing scheme is used. Besides, the consumption or operating cost/emissions penalty would only be 0.7%. This shows that differential sizing may be an excellent solution to improve the fuel cell propulsive system, but that would depend on the cost and emissions of the FCS manufacturing relative to those produced for the operation.

It is important to remark that these analyses have been done for specific driving cycles. Heavy-duty driving cycles are usually more steady than passenger car driving conditions. This explains the different durability and consumption results compared to what was obtained in previous passenger car studies [36].

6. Potential for industrial applications

The study aims to understand the current modular trend in FC heavy-duty vehicles. The obtained information not only helps to understand this kind of powertrain design but also to optimize it and combine multiple FCS so that it is possible to get a powerplant with optimum performance and durability.

The results provide valuable information for any FC truck manufacturer. On the one hand, the consumption and durability results can help companies in the heavy-duty sector estimate the total cost of their vehicles under various scenarios; therefore, knowing how the FCS size and control of their vehicles influence lifetime is very significant when trying to optimize costs in the design phase of their product. On the other hand, offering a vehicle that minimizes H_2 consumption is also a very attractive feature for any customer. Furthermore, the trade-off between performance and durability may be changed with the data in this study based on how the H_2 price changes with time.

FC heavy-duty vehicle manufacturers can use the obtained relation between consumption and durability and their knowledge about FC truck costs to improve their vehicle designs. It is important to note that the performed analyses provide some significant data that could ease the deployment of the FCHDV, thus accelerating the decarbonization of the heavy-duty transportation sector.

The vehicle used to perform the current analyses is the Hyundai XCIENT, which uses a multi-FCS composed of two FCS with 95 kW of maximum net power output (120 kW at the stack level). However, the heavy-duty transportation sector has already presented several multi-FCS trucks such as the IVECO H2Haul (2 × 100 kW), the Mercedes-Benz Gen H2 (2 × 150 kW), the VOLVO Trucks Fuel cell truck (2 × 150 kW) or the Mercedes FAUN HECTOR ENGINIUS (3 × 30 kW), but a few are commercially available. In addition, many other companies have also designed their heavy-duty fuel cell vehicle with a single FCS (Toyota-Kenworth, ESORO, or VDL) [31]. It is easy to note that the differential size design has yet to be exploited by the FC heavy-duty transportation sector, which makes the obtained results even more helpful for companies in the field. In this way, any truck manufacturer, especially those interested in multi-FCS (e.g. Hyundai, IVECO, or Mercedes-Benz), could use the data presented in the current study to improve the performance and durability features of their FC heavy-duty vehicle models. The submitted data can be helpful for manufacturers because they already know the specific driving cycle conditions their vehicle would experience typically or the ideal characteristics the proposed truck should have to match their consumer requirements. The combination of this knowledge and the information the presented results provide make any FC truck manufacturer a potential reader for the present study because they could benefit significantly from these data.

Despite the benefits the obtained data brings for the FC heavy-duty vehicle sector, it should also be noted that performance and durability are not the only characteristics of interest for manufacturers. Cost is also not considered because it is assumed that the heavy-duty company can optimize this value using the obtained data and their knowledge about this vehicle application. In this case, they could explore the trade-off between the CAPEX (influenced by the durability of the FC stacks) and the OPEX (affected by the H_2 consumption), which follow an opposite trend when limiting the FCS dynamics. However, the current decarbonization trend makes emissions important when launching any product into the market. To evaluate the use and optimization of differential control and sizing designs for heavy-duty multi-FCS correctly, performing a life cycle assessment (LCA) is essential. This study would give the manufacturer a complete understanding of the differential control and sizing designs. For this purpose, the authors intend to extend this research line in the previous terms with the following studies.

7. Research limitations, challenges, and future prospects

The present study shows that differential sizing and control could benefit a multi-FCS powertrain in terms of cost and environmental impact. Besides, this benefit cannot be quantified entirely yet. The obtained consumption and durability values can be used to measure the cost and emissions of the system. Thus, the analyzed results represent a way to reach the final quantities needed to evaluate any powertrain (TCO and LCA).

The cost of any transport means can be computed using a TCO (Total Cost of Ownership) model [53]. These calculations include the CAPEX (Capital Expenditure) and the OPEX (Operation Expenditure). The CAPEX represents the initial acquisition value of the vehicle, which comprehends the cost of the powertrain, energy storage, truck production, and depreciation over time. Besides, the OPEX represents the vehicle's operation cost, including fuel (H_2), consumption, tolls of the routes, fueling infrastructure, vehicle maintenance, and insurance. Nowadays, the cost of hydrogen-associated elements is very expensive due to their low deployment level. Therefore, any TCO, including H_2 technologies, should also include a study that measures how costs would change over the years until the full hydrogen industrialization is stated in [54]. Thus, cost calculation represents a challenge that should be studied in future projects. By using the results produced in this study, it would be possible to understand the cost in terms of both CAPEX and OPEX of a heavy-duty fuel cell vehicle depending on the design and the control dynamics, which could be beneficial to identify the optimum configuration that minimizes the costs.

The importance of hydrogen fuel cell technologies is highly related to their zero tailpipe emissions during operation time. However, emissions should be quantified in well-to-wheel terms. The LCA or Life Cycle Assessment comprises the fuel production and distribution, the vehicle manufacturing, and the operation cycle emissions. To estimate the environmental impact of this technology, a specific LCA analysis should be performed as it was done in [44] for passenger car applications.

Finally, it is important to remark that the energy management strategy selects the current value of each FCS depending on the demanded power by the driving cycle and the values that produce the minimum H_2 consumption during the cycle. The problem is that it is impossible to compute the minimum consumption value during real driving conditions because the demanded power is not known in advance. Some recent studies in the literature are already exploring alternatives to predict the power trend and optimize the management strategy in real-time operations [55].

Heavy-duty trucks follow predefined routes for transportation purposes along Europe (TENT routes). In addition, GPS-based models such as MAPBOX can predict the velocity behavior on a specific route. Thus, coupling these models with the known routes can be a solution to a power predicting model, which may lead to a redefinition of the used energy management strategy.

The mentioned matters represent important challenges to make simulations more realistic and will be considered in future studies. Solving them would take heavy-duty fuel cell vehicle deployment a step closer to becoming a reality despite their complexity.

CRediT authorship contribution statement

R. Novella: Conceptualization, Supervision, Formal analysis, Project administration, Resources, Methodology, Writing – original draft. **J. De la Morena:** Formal analysis, Supervision, Project administration. **M. Lopez-Juarez:** Investigation, Resources, Data curation, Methodology, Software, Writing – review & editing. **I. Nidaguila:** Methodology, Validation, Software, Writing – original draft.

Declaration of competing interest

The authors declare that they have no known competing financial interests or personal relationships that could have appeared to influence the work reported in this paper.

Data availability

Data will be made available on request.

Acknowledgments

This research has been partially funded by the Spanish Ministry of Science, Innovation, and University through the University Faculty Training (FPU) program (FPU19/00550) and by the Generalitat Valenciana (Conselleria d'Innovació, Universitats, Ciència i Societat Digital) as a part of the DEFIANCE research project (CIPROM/2021/039) through the PROMETEO funding program.

References

[1] European Commission. Sustainable and smart mobility strategy-putting European transport on track for the future. Tech. Rep. COM(2020) 789 final, European Union; 2020.
[2] Ragon P-L, Rodríguez F. Road freight decarbonization in Europe: Readiness of the European fleets for zero-emission trucking. Tech. Rep., The International Council for Clean Transportation (ICCT); 2022, www.clean-trucking.eu.
[3] van der Sman E, Peerlings B, Kos J, Lieshout R, Boonekamp T. Destination 2050 - A route to net zero European aviation. Tech. Rep. NLR-CR-2020-510, NLR, Royal Netherlands Aerospace Centre; 2021.
[4] Mission Innovation. Industry roadmap for zero-emission shipping mission. Tech. Rep., 2022, http://mission-innovation.net/missions/shipping/.
[5] The International Council on Clean Transportation (ICCT). Vision 2050: A strategy to decarbonize the global transport sector by mid-century. Tech. Rep., 2022, http://mission-innovation.net/missions/shipping/.
[6] Ministerio para la transición ecológica y el reto demográfico (MITERD). Hoja de ruta del hidrógeno: Una apuesta por el hidrógeno renovable. Tech. Rep., Gobierno de España; 2020, https://energia.gob.es/es-es/Novedades/Paginas/publicacion-hoja-de-ruta-del-hidrogeno-apuesta-hidrogeno-renovable.aspx.
[7] European Commission. A hydrogen strategy for a climate-neutral Europe. Tech. Rep. COM(2020) 301 final, European Union; 2020.
[8] Desantes J, Molina S, Novella R, Lopez-Juarez M. Comparative global warming impact and NOX emissions of conventional and hydrogen automotive propulsion systems. Energy Convers Manage 2020;221:113137. http://dx.doi.org/10.1016/j.enconman.2020.113137.
[9] Çabukoglu E, Georges G, Küng L, Pareschi G, Boulouchos K. Fuel cell electric vehicles: An option to decarbonize heavy-duty transport? Results from a Swiss case-study. Transp Res D 2019;70:35–48. http://dx.doi.org/10.1016/j.trd.2019.03.004.
[10] Clean Hydrogen in European Cities (CHIC). Fuel cell electric buses: A proven zero-emission solution. Tech. Rep., 2017, https://fuelcellbuses.eu/.
[11] International Energy Agency (IEA). Technology roadmap: Hydrogen and fuel cells. Tech. Rep., 2015, https://www.iea.org/reports/technology-roadmap-hydrogen-and-fuel-cells.
[12] Yu X, Sandhu NS, Yang Z, Zheng M. Suitability of energy sources for automotive application – A review. Appl Energy 2020;271:115169. http://dx.doi.org/10.1016/j.apenergy.2020.115169.
[13] Bethoux O. Hydrogen fuel cell road vehicles: State of the art and perspectives. Energies 2020;13(21). http://dx.doi.org/10.3390/en13215843.
[14] Yan J, Wang G, Chen S, Zhang H, Qian J, Mao Y. Harnessing freight platforms to promote the penetration of long-haul heavy-duty hydrogen fuel-cell trucks. Energy 2022;254:124225. http://dx.doi.org/10.1016/j.energy.2022.124225.
[15] Cunanan C, Tran M-K, Lee Y, Kwok S, Leung V, Fowler M. A review of heavy-duty vehicle powertrain technologies: Diesel engine vehicles, battery electric vehicles, and hydrogen fuel cell electric vehicles. Clean Technol 2021;3(2):474–89. http://dx.doi.org/10.3390/cleantechnol3020028.
[16] Kim Y, Han J, Yu S. Establishment of energy management strategy of 50 kW PEMFC hybrid system. Energy Rep 2023;9:2745–56. http://dx.doi.org/10.1016/j.egyr.2023.01.096.
[17] Li H, Chaoui H, Gualous H. Cost minimization strategy for fuel cell hybrid electric vehicles considering power sources degradation. IEEE Trans Veh Technol 2020;69(11):12832–42. http://dx.doi.org/10.1109/TVT.2020.3031000.
[18] Xu C, Guo K, Yang F. A comparative study of different hybrid electric powertrain architectures for heavy-duty truck. IFAC-PapersOnLine 2018;51(31):746–53. http://dx.doi.org/10.1016/j.ifacol.2018.10.136, 5th IFAC Conference on Engine and Powertrain Control, Simulation and Modeling E-COSM 2018.

[19] Morozov A, Humphries K, Zou T, Rahman T, Angeles J. Design, analysis, and optimization of a multi-speed powertrain for class-7 electric trucks. SAE Int J Altern Powertrains 2018;7:27–42. http://dx.doi.org/10.4271/08-07-01-0002.
[20] Verbruggen FJR, Silvas E, Hofman T. Electric powertrain topology analysis and design for heavy-duty trucks. Energies 2020;13(10). http://dx.doi.org/10.3390/en13102434.
[21] Kast J, Vijayagopal R, Gangloff JJ, Marcinkoski J. Clean commercial transportation: Medium and heavy duty fuel cell electric trucks. Int J Hydrogen Energy 2017;42(7):4508–17. http://dx.doi.org/10.1016/j.ijhydene.2016.12.129.
[22] Sulaiman N, Hannan M, Mohamed A, Ker P, Majlan E, Wan Daud W. Optimization of energy management system for fuel-cell hybrid electric vehicles: Issues and recommendations. Appl Energy 2018;228:2061–79. http://dx.doi.org/10.1016/j.apenergy.2018.07.087.
[23] Ravey A, Blunier B, Miraoui A. Control strategies for fuel-cell-based hybrid electric vehicles: From offline to online and experimental results. IEEE Trans Veh Technol 2012;61(6):2452–7. http://dx.doi.org/10.1109/TVT.2012.2198680.
[24] Xu L, Ouyang M, Li J, Yang F, Lu L, Hua J. Application of Pontryagin's Minimal Principle to the energy management strategy of plugin fuel cell electric vehicles. Int J Hydrogen Energy 2013;38(24):10104–15. http://dx.doi.org/10.1016/j.ijhydene.2013.05.125.
[25] Ferrara A, Jakubek S, Hametner C. Energy management of heavy-duty fuel cell vehicles in real-world driving scenarios: Robust design of strategies to maximize the hydrogen economy and system lifetime. Energy Convers Manage 2021;232:113795. http://dx.doi.org/10.1016/j.enconman.2020.113795.
[26] Peng H, Chen Z, Li J, Deng K, Dirkes S, Gottschalk J, Ünlübayir C, Thul A, Löwenstein L, Pischinger S, Hameyer K. Offline optimal energy management strategies considering high dynamics in batteries and constraints on fuel cell system power rate: From analytical derivation to validation on test bench. Appl Energy 2021;282:116152. http://dx.doi.org/10.1016/j.apenergy.2020.116152.
[27] Li H, Ravey A, N'Diaye A, Djerdir A. Online adaptive equivalent consumption minimization strategy for fuel cell hybrid electric vehicle considering power sources degradation. Energy Convers Manage 2019;192:133–49. http://dx.doi.org/10.1016/j.enconman.2019.03.090.
[28] Jain M, Desai C, Williamson SS. Genetic algorithm based optimal powertrain component sizing and control strategy design for a fuel cell hybrid electric bus. In: 2009 IEEE vehicle power and propulsion conference. 2009, p. 980–5. http://dx.doi.org/10.1109/VPPC.2009.5289740.
[29] Anselma PG, Belingardi G. Fuel cell electrified propulsion systems for long-haul heavy-duty trucks: present and future cost-oriented sizing. Appl Energy 2022;321:119354. http://dx.doi.org/10.1016/j.apenergy.2022.119354.
[30] Peng F, Xie X, Wu K, Zhao Y, Ren L. Online hierarchical energy management strategy for fuel cell based heavy-duty hybrid power systems aiming at collaborative performance enhancement. Energy Convers Manage 2023;276:116501. http://dx.doi.org/10.1016/j.enconman.2022.116501.
[31] Pardhi S, Chakraborty S, Tran D-D, El Baghdadi M, Wilkins S, Hegazy O. A review of fuel cell powertrains for long-haul heavy-duty vehicles: Technology, hydrogen, energy and thermal management solutions. Energies 2022;15(24). http://dx.doi.org/10.3390/en15249557.
[32] Sim K, Vijayagopal R, Kim N, Rousseau A. Optimization of component sizing for a fuel cell-powered truck to minimize ownership cost. Energies 2019;12(6). http://dx.doi.org/10.3390/en12061125.
[33] Cox B, Bauer C, Mendoza Beltran A, van Vuuren DP, Mutel CL. Life cycle environmental and cost comparison of current and future passenger cars under different energy scenarios. Appl Energy 2020;269:115021. http://dx.doi.org/10.1016/j.apenergy.2020.115021.
[34] Fletcher T, Ebrahimi K. The effect of fuel cell and battery size on efficiency and cell lifetime for an L7e fuel cell hybrid vehicle. Energies 2020;13(22). http://dx.doi.org/10.3390/en13225889.
[35] Liu C, Liu L. Optimal power source sizing of fuel cell hybrid vehicles based on Pontryagin's minimum principle. Int J Hydrogen Energy 2015;40(26):8454–64. http://dx.doi.org/10.1016/j.ijhydene.2015.04.112.
[36] Molina S, Novella R, Pla B, Lopez-Juarez M. Optimization and sizing of a fuel cell range extender vehicle for passenger car applications in driving cycle conditions. Appl Energy 2021;285:116469. http://dx.doi.org/10.1016/j.apenergy.2021.116469.
[37] Desantes J, Novella R, Pla B, Lopez-Juarez M. A modeling framework for predicting the effect of the operating conditions and component sizing on fuel cell degradation and performance for automotive applications. Appl Energy 2022;317:119137. http://dx.doi.org/10.1016/j.apenergy.2022.119137.
[38] Desantes J, Novella R, Pla B, Lopez-Juarez M. Effect of dynamic and operational restrictions in the energy management strategy on fuel cell range extender electric vehicle performance and durability in driving conditions. Energy Convers Manage 2022;266:115821. http://dx.doi.org/10.1016/j.enconman.2022.115821.
[39] Hyundai Motor Company. World's first fuel cell heavy-duty Truck, Hyundai XCIENT Fuel Cell, heads to Europe for commercial use. Hyundai Mot Co Brand J 2020. https://fuelcellsworks.com/news/worlds-first-fuel-cell-heavy-duty-truck-hyundai-xcient-fuel-cell-heads-to-europe-for-commercial-use/.
[40] Murschenhofer D, Kuzdas D, Braun S, Jakubek S. A real-time capable quasi-2D proton exchange membrane fuel cell model. Energy Convers Manage 2018;162:159–75. http://dx.doi.org/10.1016/j.enconman.2018.02.028.
[41] Springer TE, Zawodzinski TA, Gottesfeld S. Polymer electrolyte fuel cell model. J Electrochem Soc 1991;138(8):2334. http://dx.doi.org/10.1149/1.2085971.
[42] Corbo P, Migliardini F, Veneri O. Experimental analysis and management issues of a hydrogen fuel cell system for stationary and mobile application. Energy Convers Manage 2007;48(8):2365–74. http://dx.doi.org/10.1016/j.enconman.2007.03.009.
[43] Corbo P, Migliardini F, Veneri O. Experimental analysis of a 20kWe PEM fuel cell system in dynamic conditions representative of automotive applications. Energy Convers Manage 2008;49(10):2688–97. http://dx.doi.org/10.1016/j.enconman.2008.04.001.
[44] Desantes J, Novella R, Pla B, Lopez-Juarez M. Impact of fuel cell range extender powertrain design on greenhouse gases and NOX emissions in automotive applications. Appl Energy 2021;302:117526. http://dx.doi.org/10.1016/j.apenergy.2021.117526.
[45] Onori S, Serrao L, Rizzoni G. Hybrid electric vehicles: Energy management strategies. London: Springer; 2016, http://dx.doi.org/10.1007/978-1-4471-6781-5.
[46] Luján JM, Guardiola C, Pla B, Reig A. Cost of ownership-efficient hybrid electric vehicle powertrain sizing for multi-scenario driving cycles. Proc Inst Mech Eng D 2016;230:382–94. http://dx.doi.org/10.1177/0954407015586333.
[47] Pei P, Chang Q, Tang T. A quick evaluating method for automotive fuel cell lifetime. Int J Hydrogen Energy 2008;33:3829–36. http://dx.doi.org/10.1016/j.ijhydene.2008.04.048.
[48] Knights S. 6 - Operation and durability of low temperature fuel cells. In: Hartnig C, Roth C, editors. Polymer electrolyte membrane and direct methanol fuel cell technology. Woodhead publishing series in energy, vol. 1, Woodhead Publishing; 2012, p. 137–77. http://dx.doi.org/10.1533/9780857095473.2.137.
[49] Kangasniemi KH, Condit DA, Jarvi TD. Characterization of vulcan electrochemically oxidized under simulated PEM fuel cell conditions. J Electrochem Soc 2004;151(4):E125. http://dx.doi.org/10.1149/1.1649756.
[50] Bi W, Fuller T. Temperature effects on PEM fuel cells Pt/C catalyst degradation. ECS Trans 2007;11(1):1235. http://dx.doi.org/10.1149/1.2781037.
[51] Dutta MM, Jia N, Lu S, Colbow V, Wessel S. Effects of upper potential dwell time, transients and relative humidity on PEM fuel cell cathode catalyst degradation. ECS Meet Abstr 2010;MA2010-01(9):543. http://dx.doi.org/10.1149/MA2010-01/9/543.
[52] Popovich N. 2015 annual progress report: DOE hydrogen and fuel cells program. Tech. Rep. NREL/BK-6A10-64753; DOE/GO-102015-4731, 2015.
[53] Hu M, Zhao B, Suhendri S, Cao J, Wang Q, Riffat S, Yang R, Su Y, Pei G. Experimental study on a hybrid solar photothermic and radiative cooling collector equipped with a rotatable absorber/emitter plate. Appl Energy 2022;306:118096. http://dx.doi.org/10.1016/j.apenergy.2021.118096.
[54] H2Accelerate. Analysis of cost of ownership and the policy support required to enable industrialisation of fuel cell trucks. Tech. Rep., 2022, https://h2accelerate.eu/.
[55] Zhou Y, Ravey A, Péra M-C. Multi-objective energy management for fuel cell electric vehicles using online-learning enhanced Markov speed predictor. Energy Convers Manage 2020;213:112821. http://dx.doi.org/10.1016/j.enconman.2020.112821.